Fluorinated Polypropylene Barrier Materials: Preparation and Characterization

Si Cheng, Dijiang Wen

College of Chemistry, Chemical Engineering and Materials, Soochow University, Suzhou 215123, People's Republic of China

Received 11 January 2009; accepted 7 August 2009
DOI 10.1002/app.31248
Published online 28 January 2010 in Wiley InterScience (www.interscience.wiley.com).

ABSTRACT: A series of novel fluorinated polypropylenes (FPP) with low surface tension were prepared by reactive extrusion of polypropylene (PP) with fluorinated methacrylate, 2,3,4,5,5,5-hexafluoro-2,4-bis (trifluoromethyl) pentyl methacrylate (HFPMA), aiming at improving the barrier properties of the material for the containers of organic liquids. The surface characteristics of these polypropylene materials and the influence of HFPMA on the crystalline behavior were investigated by the X-ray photoelectron spectroscopy (XPS) and wide-angle X-ray diffraction (WAXD). The surface tension of the FPPs is found to be in the range of 28.8–22.9 mN/m while varying the fluorinated monomer contents, which was lower than that of the original PP (about 30 mN/m). The barrier properties of these materials as the containers were studied by using blow-molded bottles made of FPP and PP. The results showed that enhanced permeation resistance for acetone and xylene solvents as well as better antiultraviolet transmittance properties were achieved in FPP bottles. The acetone and xylene permeation ratio of the FPP bottles were about 1.62 and 1.28 times compared to that of PP bottles, respectively. In addition, the WAXD and DSC studies suggested that the grafting of the fluorinated methacrylate, HFPMA, onto the PP might induce the formation of β form crystals, which is rarely found in the common PP materials. The percentage of β form crystals reached 33.6%, estimated by WAXD, in the FPP with 20% (by weight) of HFPMA. © 2010 Wiley Periodicals, Inc. J Appl Polym Sci 116: 2793–2801, 2010

Key words: fluoropolymers; poly(propylene); barrier; reactive extrusion

INTRODUCTION

Many common polymer materials, such as polyethylene (PE) and polypropylene (PP), have been used as the major materials for the automotive fuel tanks, vessels for storage of toxic and volatile liquids, pipes for transfer of liquids for the last several decades because of their cheapness and easiness for processing. However, it is also well known that the PE and PP are permeable for many organic solvents such as toluene, xylene, acetone, and gasoline. Therefore, considerable research interest has been devoted to the development of polymeric materials with barrier properties to the organic liquids. These materials will be very useful in reducing the permeability of the organic solvent and gasoline and thus of great significance in reducing the environment pollution.[1,2]

There have been several methods to prepare the barrier materials in the literature, such as surface fluorination[3–8] or surface sulfonation,[9–12] multilayer coextrusion technique,[13–16] and laminar blend technique.[2,17–20] Among them, the multilayer coextrusion and laminar blend techniques were usually used for improving material barrier properties, while the blending of two or more polymer materials is necessary in these process techniques which might cause some problems, such as comparability between the two polymers. Surface fluorination of polymers is a heterogeneous reaction of gaseous F_2 with a polymer surface and, therefore, only the outside surface layer is modified (0.01–10 μm). Fluorinated polymers have been paid numerous attentions because of their unique properties, such as low surface energy, low wettability, better hydrophobicity and oleophobicity enhanced chemical stability, and good barrier properties.[21–30] The direct surface fluorination is very promising for improving the barrier properties of these materials as automotive polymer fuel tanks and vessels for storage of toxic and volatile liquids in the industry,[31–33] while it has not been widely used in the polymer process due to the complex equipment, environmental and healthcare concerns. The reactive extrusion, a widely used technique in the polymer process, is very practical for introducing the functional groups onto PP. Polyolefin have been proven to be preferred substrates for the reactive extrusion technique because of their ready availability, low cost, and widespread commercial application.

Correspondence to: D. Wen (wendijiang@suda.edu.cn).

The chemical modification of PP has been widely studied, such as modificated with acrylates,[34] glycidyl methacrylate,[35,36] and maleic anhydride.[37] The mechanism, the control reactive condition, and process rheology during the reactive extrusion process have been investigated in detail.[38] However, much less attention has been paid on the chemical modification of PP with fluorinated methacrylates.

In this study, a series of fluorinated polypropylenes (FPPs), with low surface tension and improved barrier and antiultraviolet transmittance properties, were prepared by reactive extrusion. These materials can be widely used in automotive polymer fuel tanks and vessels for the storage of toxic and volatile liquids. Moreover, the possible reasons for the improvement in the barrier properties were also investigated. It was found that the grafting the fluorinated methacrylate, 2,3,4,5,5,5-hexafluoro-2,4-bis (trifluoromethyl) pentyl methacrylate (HFPMA), onto PP with twin-screw extrude decreased the surface tension of polypropylene and induced the formation of β form crystal, which is rarely found in the common PP materials.

This article presents our work on the preparation, surface characterization, crystalline behavior of polypropylene with and without fluorinated methacrylate, as well as their rheological properties, antiultraviolet transmittance properties, and barrier properties. The relationship between the specific structure in FPP and the improved barrier properties is also discussed in detail.

EXPERIMENT

Materials

Polypropylene (PP-2401) was offered by Yanshan Petroleum Chemical company in Beijing, density = 0.90–0.91 g/cm^3, melt index = 3 g/10 min (190°C, 2160 g); 2,3,4,5,5,5-hexafluoro-2,4-bis (trifluoromethyl)pentyl methacrylate (HFPMA) (liquid, boiling point = 170°C; purity = 98–99%; surface tension = 18 mN/m) was offered by XeoGia Fluorine-Silicon Chemical company. HFPMA is a monomer of methacrylates having high fluorine content and high branched chain structure, as shown in Scheme 1.

The free radical initiator, dicumyl peroxide (DCP), with a half-lifetime ($t_{1/2}$) of 9.2 min at 150°C and a purity of 90%, was supplied by Shanghai Zhongli chemical company. Styrene (St) was used to inhibit the degradation of PP and improve the grafting ratio.[39–42]

Sample preparation

PP, DCP(0.5%), styrene (St) (5%), and HFPMA (10%, 15%, 20%) were dry-mixed at high speed mixer (SHR-10, Zhang Jiagang Light Industry Machine Corporation) at room temperature, and then were melt-mixed in a corotating twin-screw extruder (Φ = 36 mm, L/D = 40, SHJ-36, the Chengmeng company, Nanjing) with the screw speed fixed at 75 rpm, and zone temperature of 165°C/170°C/175°C/180°C/180°C/190°C/190°C/200°C/190°C were used. The resulting grafted PPs were cut into small particles for further characterizations.

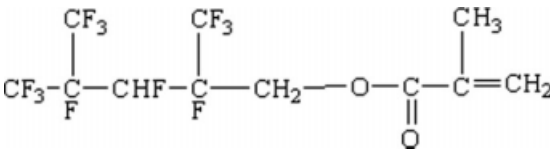

Scheme 1 Chemical structure of HFPMA.

The PPs and FPPs were prepared from the twin screw extruder and were dried at 80°C for 16 h and then were blow-molded in a XS-ZY-125B extrusion-blow-molding machine (from Changjiang Plastic Machine Corporation, Changzhou, China), with an extrusion temperature of 190°C and a screw speed of 600 rpm. The weight of blow-molded bottles is about 13 g and the capacity is about 100 mL. The wall thickness of blow-molded bottles is about 1 mm, and the bottom thickness is about 1.5 mm.

Characterization

Purification and characterization of FPP

It is easy to produce byproduct during the reactive extrusion process. Therefore, the grafted polypropylenes need to be purified in order to remove the homopolymer, nongrafted monomer, and other byproducts as also suggested in the related literature.[34–37] The purification process for the materials was carried out according to the following procedure.

The FPP samples by twin-screw extruder were dissolved in refluxing xylene with a concentration of 1% (wt (g)/vol (mL)), and then were precipitated in excess acetone. The resulting polymers were filtered, washed, and dried under vacuum at 80°C for 24 h. Then the products were hot-pressed under 190°C into a piece of thin film and analyzed by FTIR (NICOLET 5700, American thermocorporation). The FTIR spectra were recorded from the compressed thin disk in analytical-grade KBr power.

Surface analysis by X-ray photoelectron spectroscopy

The purified FPP was sent to do XPS analyses. The surface component analysis of sample was carried out by XPS (Sigma Probe of VA Company, Britain) with a condition of 10 scans, 1 m 10.5 s, by Beijing

Research Institute of Chemical Industry. The FPP was etched by argon ion etch technique, and the etched depth was about 50 nm.

Wide-angle X-ray diffraction

The purified samples were hot-pressed into sheets with a thickness of 1 mm in a plate press machine. The specimens with a dimension of 1 mm × 1 mm were scanned from 5° to 50° by wide-angle X-ray diffraction. Wide-angle X-ray diffraction was measured on a PW1700 X-ray diffractometer. The relative content of β-modification was estimated from the *K*-values of the samples, which was calculated according to the following equation[43]

$$K_\beta = \frac{I_{(300)\beta}}{I_{(300)\beta} + I_{(110)\alpha} + I_{(040)\alpha} + I_{(130)\alpha}} \quad (1)$$

where $I_{(300)\beta}$ is the diffraction intensity of the β(300) plane at diffraction angle $2\theta = 16.08°$ and $I_{(110)\alpha}$, $I_{(040)\alpha}$, $I_{(130)\alpha}$ are the diffraction intensities of the α(110), α(040), and α(130) planes at diffraction angles $2\theta = 14.08°$, 16.81°, 18.46°, respectively.

The α-form crystallinity degree (X_c) of PP can also be calculated, according to the following experience equation.[43]

$$X_{c(\alpha)} = \frac{I_c}{I_C + 1.25I_A} \times 100\% \quad (2)$$

$$I_C = I_{110} + 1.63I_{040} + 2.14I_{130} + 3.51I_{041}^{111} \quad (3)$$

The total crystallinity of α-form crystal and β-form crystal are defined by the following equation,

$$X_{C(\alpha+\beta)} = \frac{I_C + I_{(300)}}{I_C + 1.25I_A + I_{(300)}} \times 100\% \quad (4)$$

where I_c is the integral intension of the crystalline region, I_A is the integral intension of the amorphous region. I_{110}, I_{040}, I_{130}, and $I^{111}{}_{140}$ denote the integral intensions of (110), (040), (130), (111), and (041, $\bar{1}$31) crystal plane, respectively. $I_{(300)}$ is the integral intension of (300) crystal plane of β-form crystal.

Calculation of the surface tension

The surface tension of the sample was calculated from the contact angles of the PP and purified FPP according to eqs. (5) and (6) as shown below. The static contact angles were measured by JC2001-C1 static contact angles apparatus (Zhongchen technique instrument company, Shanghai). Equations (5) and (6) were deduced from the surface tension component approach, which was advanced by Owens and Wendt[44] in 1969. The surface tension was considered to have two components in this approach, the apolar components and polar components.

TABLE I
Surface Tension and Components of Water and Ethylene Glycol (20°C)

	Surface tension (mN/m)		
Probe liquid	γ_l	$\gamma_l{}^d$	$\gamma_l{}^p$
Water	72.8	21.8	51
Ethylene glycol	48	29	19

$$\cos\theta = \frac{2}{\gamma_l}\left[\left(\gamma_l^d\gamma_s^d\right)^{1/2} + \left(\gamma_l^p\gamma_s^p\right)^{1/2}\right] - 1 \quad (5)$$

$$\gamma_s = \gamma_s^d + \gamma_s^p \quad (6)$$

where γ_l denotes the surface tension of liquid–gas, $\gamma_l{}^d$, $\gamma_l{}^p$ refer the apolar and polar component of this liquid, respectively. And γ_s denotes the surface tension of solid–gas, $\gamma_l{}^d$, $\gamma_l{}^p$ refer the apolar and polar component of the liquid-gas. θ is the contact angle. The value of γ_l, $\gamma_l{}^d$, and $\gamma_l{}^p$ of water and ethylene glycol at 20°C are listed in the Table I. Therefore, the surface tension of solid can be easily obtained, once the contact angle is measured.

DSC analysis

The crystallization process was investigated using a Perkin-Elmer Diamond differential scanning calorimeter under nitrogen. The samples were scanned from room temperature to 200°C with a heating rate of 10°C /min, and then the temperature was held at 200°C for 5 min to remove the thermal history effects. Afterwards the samples were cooled to 50°C with a rate for 10°C /min, followed by reheating the samples from 50 to 200°C with a rate of 10°C /min.

Rheological properties

The purified samples were pressed into sheets with a thickness of 1 mm and cut into a circle plate with a diameter of about 30 mm. Rheological properties were investigated by using a rotational rheometer (TA Instruments, AR-2000). The rheological curves of PP and FPPs were measured.

Permeation properties of the blow-molded bottles

The barrier properties of the blow-molded bottles were evaluated by measuring the weight loss of polar solvents, acetone, and nonpolar solvents, xylene, which were filled in the bottles depending on the ASTM D2684-89. The bottles were initially

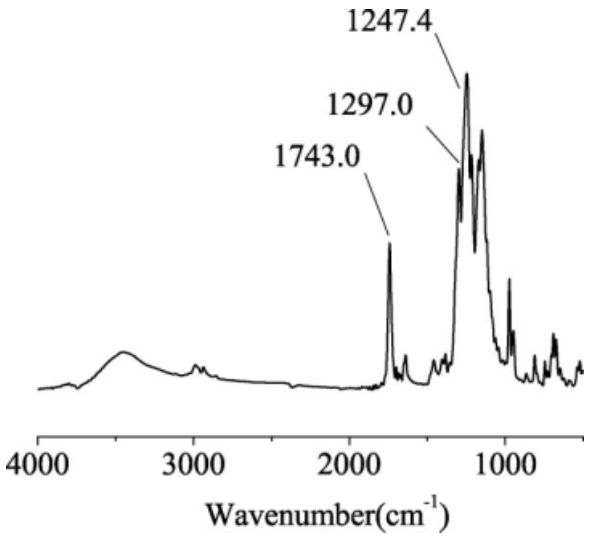

Figure 1 FTIR spectra of HFPMA.

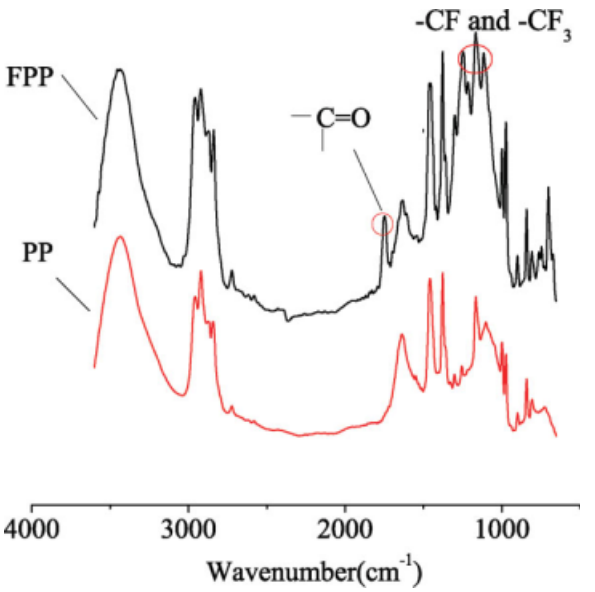

Figure 2 FTIR spectra of PP and FPPs. [Color figure can be viewed in the online issue, which is available at www.interscience.wiley.com.]

filled with about 100 g acetone or xylene. The weight loss of acetone or xylene was determined after placing the filled bottles in an air-circulating chamber at 40°C for 14 days.[20] The permeation rate for bottles of each type was reported as the average value from at least three to five bottles made of the same material.

Antiultraviolet transmittance properties

The ultraviolet spectrum of HFPMA was measured by ultraviolet spectrophotometer (UV-3010, Hitachi Instruments, Japan).

The transmittance of ultraviolet radiation of PP and FPPs were measured by UV protection factor instrument (UV-1000F, American Labsphere Instrument).

RESULTS AND DISCUSSION

Surface structure analyses

Figure 1 showed the FTIR spectra of HFPMA, the absorption at the 1743.0 cm^{-1} could be attributed to the stretching vibration of carbonyl group (C=O). The peaks at 1297 $cm^{-1}$and 1247.4 cm^{-1} could be attributed to the stretching vibrations of —CF_3 and —CF—, respectively. These typical bands from HFPMA still exist in the spectra of FPP (Fig. 2), such as 1727 cm^{-1} for carbonyl group, 1246cm^{-1} for —CF_3 and —CF— group.

A broad scan XPS spectrum of untreated polypropylene, in Figure 3, confirmed the presence of fluorine group. After grafting HFPMA, the propylene units at the surface of the material were replaced by a complex structure with fluorine group. The carbon 1s XPS spectrum was shown in Figure 4. The band around 294.1, 289.7, and 286.4 eV could be attributed to the carbon in the —CF_3 group, —CF— bound to the —CF_3 and the —CHF— bound to —CF—, respectively.

The FPP was etched about 50 nm by argon ion etch technique. The F 1s XPS spectra of etch and unetch surface were shown in Figure 5. Results showed that the F 1s signal had a weaker intensity after the surface etching than that of no etching. In the other words, the fluorine content at various sites of polypropylene film might be different. The closer to surface, the higher fluorine content could be, which was consistent with the enrichment and aggregation of the fluorine element.[45–47]

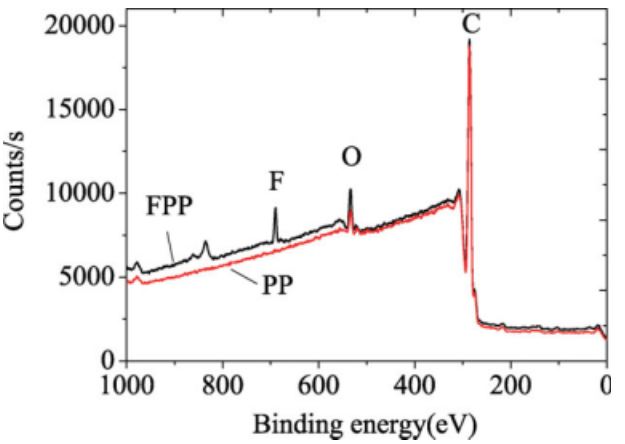

Figure 3 Broad scan XPS spectrum of PP and FPP. [Color figure can be viewed in the online issue, which is available at www.interscience.wiley.com.]

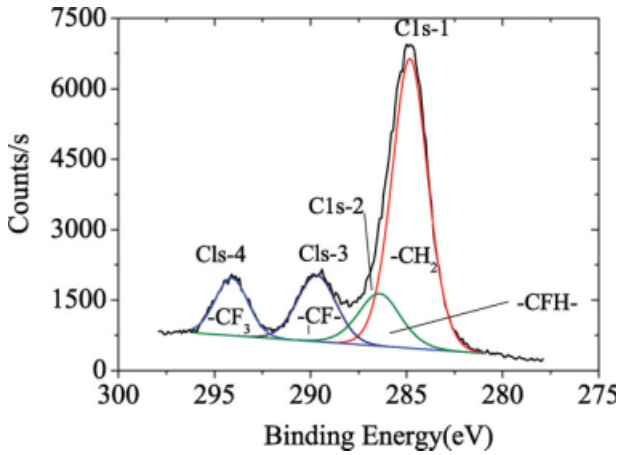

Figure 4 Carbon 1s XPS spectrum of FPP. [Color figure can be viewed in the online issue, which is available at www.interscience.wiley.com.]

Surface wettability

The static contact angles of ethylene glycol and water on the PP surface, as the content of fluorinated monomer, HFPMA, were shown in Table II. It was found that the θ values of water and ethylene glycol on the FPPs increased with the increase in the content of fluorine monomer. It could be attributed that the length of the fluorinated side chain had considerable effect on its crystal structure at the surface of polymer. In addition, the stack density of $-CF_3$ group at outer layer of the polymer was also influenced by the fluorinated side chains. The rearrangement of the fluorinated unit on the surface during the formation of fluorinated polymer was facilitated by relatively long chains.[45–47] Therefore, the contact angle would increase with increasing the content of fluorinated group.

The surface tensions of the materials were calculated according to eqs. (5) and (6), which was shown in Figure 6. It was found that PP has a lower surface tension, after grafting with HFPMA. The surface tension reached 22.9 mN m^{-1}, which is close to that of polytetrafluoroethylene (PTFE), about 18.5 mN m^{-1}.

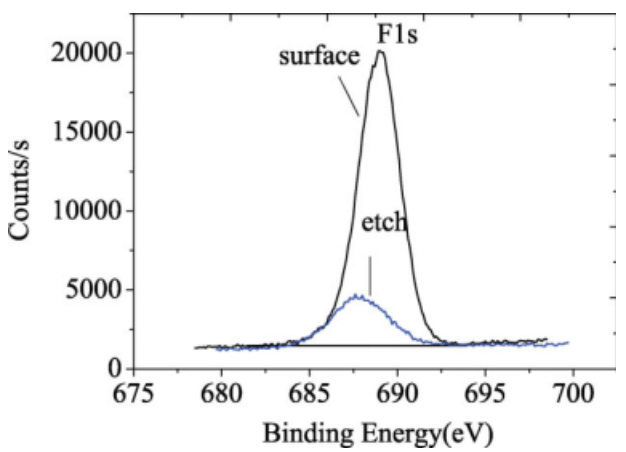

Figure 5 Fluorine 1s XPS spectrum at no-etched and etch surface of FPP. [Color figure can be viewed in the online issue, which is available at www.interscience.wiley.com.]

TABLE II
Water and Ethylene Glycol Static State Contact Angles on PP and FPPs (20°C)

	Static state contact angles	
Sample	Water	Ethylene glycol
Pure PP	102	72
FPP10	105.8	76
FPP15	106.5	78
FPP20	107	80

Crystalline behavior

The X-ray diffraction was used to investigate the crystalline structure of PP and FPP. The XRD spectra of PP and FPPs were shown in Figure 7. The assignment of the crystal plane to the different diffraction peaks were also shown in Figure 7. The four main diffraction peaks of PP were at 2θ equal to 14.08°, 16.81°, 18.46°, 21.06°, and 21.80°, as (110), (040), (130), (111), and (041, $\bar{1}31$) crystal planes, respectively, which are the typical α-form monoclinic structure of PP. The two main diffraction angles of β-form hexagonal structure were at 16.08° and at 21.20°, as (300) and (130) crystal planes, respectively. Especially, the (300) crystal plane which could be assigned to β-form crystal emerged after the grafting, and the intensity increased with the increasing the HFPMA content. It suggested that the FPPs had mixed crystal structures that is the α-form coexisted with β-form crystals.

Depending on the literature,[48] the 2θ value of noncrystal peak is at 16.30°. Therefore, the crystallinity

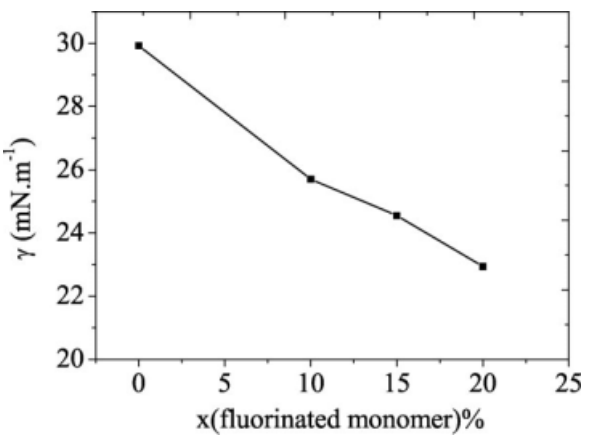

Figure 6 Effect of the content of HFPMA on surface tension of FPPs.

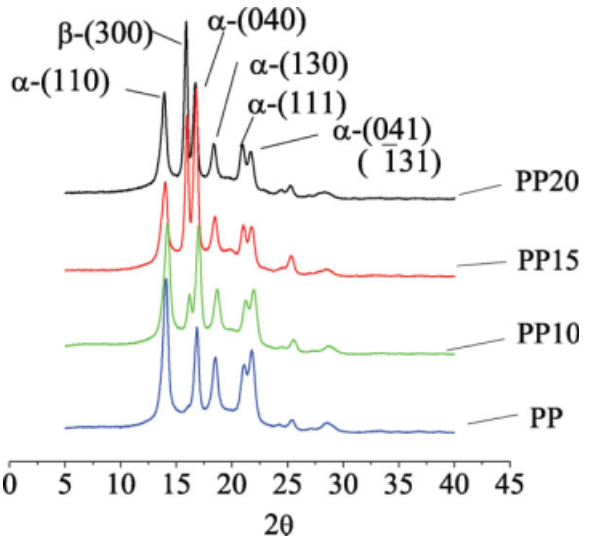

Figure 7 XRD spectra of PP and FPPs. [Color figure can be viewed in the online issue, which is available at www.interscience.wiley.com.]

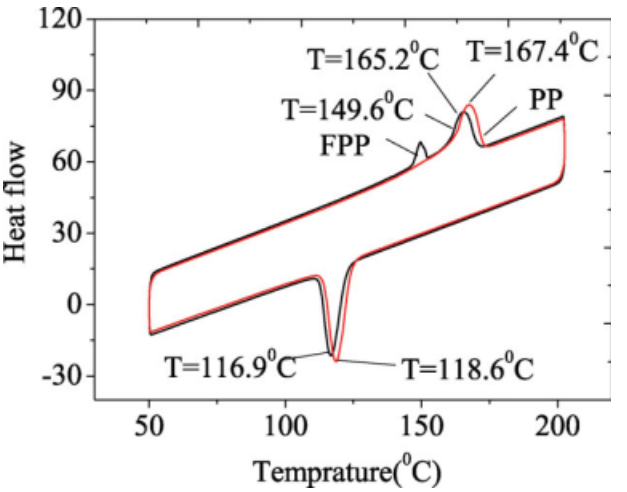

Figure 8 The DSC curves of PP and FPP20. [Color figure can be viewed in the online issue, which is available at www.interscience.wiley.com.]

of α-form and β-form were calculated according to the eqs. (2) and (4) and listed in Table III.

The data showed that the crystallinity decreased while the relative content of β form crystal, K_β (%), increased with the increasing of fluorinated methacrylate content. The relative content of β form obtained by WAXD reached 33.6% in a FPP containing 20% (by weight) of the fluorinated methacrylate.

The DSC curves of PP and FPP20 for the heating and cooling process were shown in the Figure 8. Basically, there is no significant change in the melting point (167.4 to 165.2°C), neither in the crystallization temperature (from 118.6 to 116.9°C) by introducing the fluorinated groups. However, it is worthy noting that the FPP has two melting peaks at 165.2 and 149.6°C, which could be attributed to the melting of the α-crystals and β-crystals, respectively.[49,50] Therefore, conclusion can be made that two forms of the crystals, α phase and β phase crystals, coexist in the material after grafting HFPMA. In addition, the existence of many C—F groups in the side chain account for the decrease in the melting point.

It has been reported[51–53] that β-form lamellar crystals exhibited neither the peculiar lath-like form nor the cross-hatched lamellar morphology of α-form i-PP crystals. β-form lamellar crystals were consistently observed to show an extended sheet morphology characterized by frequent giant screw dislocations. This kind of lamellar morphology and screw dislocations of β-form crystals favors for increasing the tortuosity of path during the solvent permeation.[54]

TABLE III
The Crystallinity and Relative Content of β-crystal of PP and FPP20

Sample		PP	FPP10	FPP15	FPP20
Degree of crystallinity	X_c (α)	79.4	72.2	71.9	68.6
relative content	X_c (α + β)	79.4	74.4	74.0	71.8
of β-crystal	K_β(%)	0	24.6	25.9	33.6

Rheological properties

The influence of fluorinated monomer content on the steady shear viscosity of PP and FPPs is shown in Figure 9. The PP and FPPs exhibited a non-Newtonian behavior and shear thinning behavior within all shear rate ranges. The steady shear viscosity increased with the increase in the fluorinated monomer content at the low shear rate. It meant that in the lower shear ratio, the FPPs had some extent

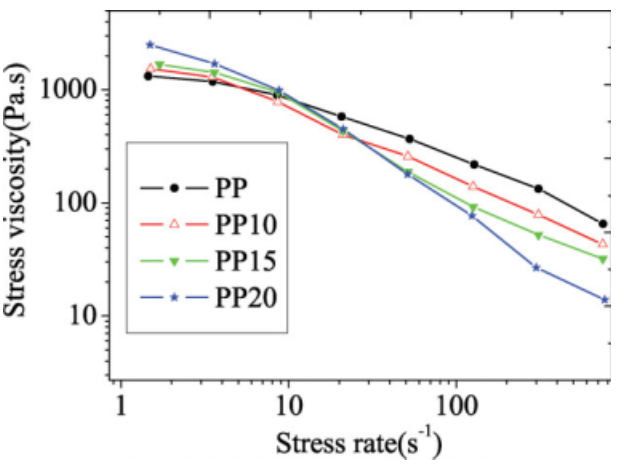

Figure 9 Effect of fluorinated monomer content loading on the steady shear viscosities of PP and FPPs. [Color figure can be viewed in the online issue, which is available at www.interscience.wiley.com.]

TABLE IV
Acetone and Xylene Permeation Rate of the PP and FPP Blow-Molded Bottles

Sample	Permeation rate (g/d)		
	Acetone	Xylene	SD (%)
PP	0.84	4.12	99.1
FPP20	0.52	3.23	99.5

segment entanglement because of the long fluorinated branch chain existing after grafting, and the more entanglement point, the higher shear viscosity.

However, the shear viscosities of all FPPs samples decreased faster than that of PP at the high shear rate. In addition, the more fluorinate monomer, the lower shear viscosity. It suggested that the FPPs showed better shear sensitivity behavior as fluorinate monomer increased. It could be explained that the high shear rate destroyed the segment entanglement and molecular interaction among the polymer chain.

Barrier properties

Barrier properties of the blow-molding bottles of the PP and FPP were evaluated by measuring the permeability of acetone and xylene through the thin wall of the bottles. There, FPP20 was chosen to blow bottles due to its lowest surface tension. The permeation ratios of acetone and xylene were shown in Table IV. As expected, the PP bottle exhibited poor barrier property for acetone and xylene, with a permeation rate of about 0.84 g/day and 4.12 g/day, respectively. However, the FPP20 bottle exhibited better permeation resistance for acetone and xylene, with a permeation rate of about 0.52 g/day and 3.23 g/day, respectively. The improvement of permeation resistance could be explained by the following several reasons.

Firstly, the surface tension of FPP20 in many cases was reduced compared to the pure PP, as mentioned in previous section (see "Surface Wettability" section), which lead to the wettability of PP decrease and that the liquids were not easy to spreading at FPP surface. At the same time, it could be found that the fluorine exited at FPP surface, as mentioned in "Surface Structure Analyses" section, and the surface fluorinated layer induced the hydrophobic and oleophobic character of FPP.[7,31–33] In addition, the fluorinated polar group led to the stronger intermolecular interaction, and more tightly chain segment arrangement. At last, the solvent permeation process is usually according to the dissolve-diffusion model. Permeability is the product of diffusivity and solubility. Therefore, reductions in diffusivity will also reduce permeability. The β form lamellar crystals exhibit neither the peculiar lath-like form nor the crosshatched lamellar morphology, which are consistently observed to show an extended sheet morphology characterized by frequent giant screw dislocations.[51–53] This kind of lamellar morphology and screw dislocations of β-form crystals favors for increasing the tortuosity of path during the solvent permeation.[54] Therefore, the permeability of low polarity organic liquids in FPP20 was reduced accordingly.

As shown in Table IV, the amount of polar acetone solvent permeated through the PP bottle is relatively smaller, compared to that of nonpolar xylene solvent. The acetone and xylene permeation ratio of the FPP20 bottles is about 1.62 and 1.28 times, respectively, slower than that of PP bottles. It is generally recognized that the nonpolar PP can allow the nonpolar solvent molecules to easily enter into and permeate through its amorphous regions.[20,55,56]

Ultraviolet transmittance properties

Usually, sun's radiation reaching earth's surface has an energy varying from 600 to 300 kJ mol^{-1}(UV light) and from 300 to 170 kJ mol^{-1}(visible light). The absorption energy of UV light would be so strong enough to cause chemical chain on scissions, thereby accelerating polymer and solvent degradation.[57] So, the polymer tanks and vessels for storage organic solvent or polymer packaging container often need to add some organic or inorganic ultraviolet absorber in order to prevent more ultraviolet penetration.[58]

Figure 10 showed the ultraviolet absorption spectrum of HFPMA. From Figure 9, it could be found that there existed strong absorption at 200 to 300 nm, which belonged to near ultraviolet region. The peak at 210 nm could be attributed to the

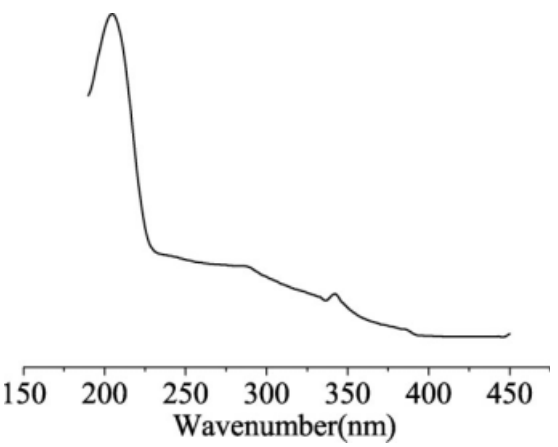

Figure 10 The ultraviolet absorption spectrum of HFPMA.

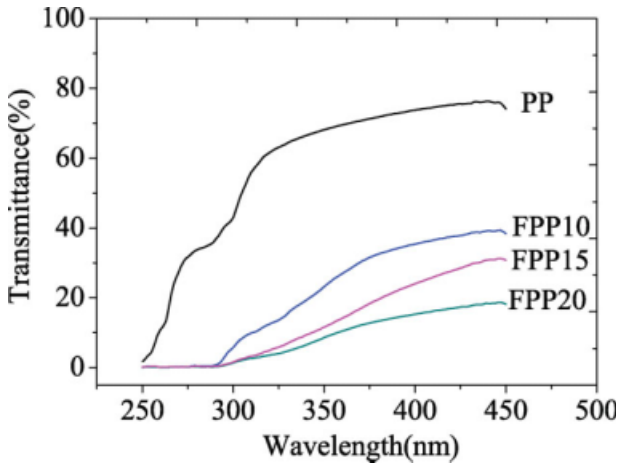

Figure 11 The ultraviolet radiation transmittance of PP and FPPs. [Color figure can be viewed in the online issue, which is available at www.interscience.wiley.com.]

absorption of acrylate group.[59] It meant that HFPMA had an ability to absorb the ultraviolet radiation.

Figure 11 showed the ultraviolet transmittance of PP and FPPs. It can be found that the ultraviolet radiation transmittance was high, from 35 to 75%, at the wavelength of ultraviolet radiation through aerosphere, from 290 to 400 nm, whereas the transmittance of FPPs had obviously decreased and the transmittance decreased with the fluorine content increasing. Specially, the transmittance of ultraviolet radiation was below 10% for FPPs at about 300nm. At 400 nm, the transmittance of PP20 only reached 15%, which was lower than that of PP. So, it could be concluded that the FPPs had better antiultraviolet transmittance properties than PP.

CONCLUSIONS

This study showed that fluorinated methacrylate, HFPMA, reduced the surface tension of polypropylene, changed the crystalline behavior of PPs, and induced the formation of β form crystal when being melt grafted onto polypropylene The XPS spectra of FPP confirmed the existence of fluorine group. In addition, it was found that the fluorine groups were enriched on the air/polymer interface. The surface tension of FPP were in the range of 28.8–22.9 mN/m while varying the fluorinated monomer content, which is smaller than the untreated polypropylene (= 30 mN/m).The relative content of β form crystal increased with the content of HFPMA increasing, reached 33.6% in a PP containing 20% (by weight) of HFPMA estimated by WAXD. In addition, the stress viscosity increased with increasing the fluorinated monomer content at the low stress rate, while the viscosity for all sample became close at the high shear rate. The barrier property for FPP has been significantly improved in the case of acetone and xylene as the solvents. The permeation rate is about 0.52 g/day and 3.23 g/day, whereas the permeation rate of the PP bottle is about 0.84 g/day and 4.12 g/day, respectively, The permeation ratio of polypropylene improved 1.62 and 1.28 times for acetone and xylene, respectively, after grafting HFPMA in twin-screw extrude. In addition, there existed a strong ultraviolet absorption peak at 210 nm in ultraviolet absorption spectrum of HFPMA, which induced that the FPPs bottles showed better antiultraviolet transmittance properties than PP.

The authors thank Dr. Li-Juan Fan for useful discussion and Beijing Research Institute of Chemical Industry for certain technical support.

References

1. Jarus, D.; Hiltner, A.; Baer, E. Polymer 2002, 43, 2401.
2. Faisant, J. B.; Aït-Kadi, A.; Bousmina, M.; Deschěnes, L. Polymer 1998, 39, 533.
3. Eschwey, M.; Van Bonn, R.; Neumann, H. U.S. Pat. 5,073,231 (1991).
4. Eschwey, M.; Van Bonn, R.; Neumann, H. U.S. Pat. 4,869,859 (1989).
5. Masson, D.; Obsomer, M. U.S. Pat. 5,213,734 (1993).
6. Hobbs, J. P. U.S. Pat. 5,244,615 (1993).
7. Kharitonov, A. P. Prog Org Coat 2008, 61, 192.
8. Marais, S.; Métayer, M.; Labbé, M.; Valleton, J. M.; Alexandre, S.; Saiter, J. M.; Poncin-Epaillard, F. Surf Coat Technol 1999, 122, 247.
9. K Mauritz, K. A.; Blackwell, R. I.; Beyer, F. L. Polymer 2004, 45, 3001.
10. Yang, B.; Manthiram, A. Electrochem Commun 2004, 6, 231.
11. Walles, W. E.; Tomkinson, D. L. U.S. Pat. 5,030,399 (1991).
12. Walles, W. E. U.S. Pat. 4,775,587 (1988).
13. Prakash, O.; Moitra, A. Comput Mater Sci 2006, 37, 12.
14. Elyashevich, G. K.; Rosova, E. Y.; Kuryndin, I. S. Desalination 2002, 144, 21.
15. Yoon, C. B.; Lee, S. H.; Lee, S. M.; Kim, H. E. J Eur Ceram Soc 2006, 26, 2345.
16. Castle, G. J.; Shih, D. R.; Bushman, K. S.; Craig, A. U.S. Pat. 6,582,808 (2003).
17. Lohfink, G. W.; Kamal, M. R. Polym Eng Sci 1993, 33, 1404.
18. Jyongsik, J.; Lee, D. K. Polymer 2004, 45, 1599.
19. Huang, C. H.; Wu, J. S.; Huang, C. C. J Polym Res 2004, 11, 75.
20. Cui, X. G.; Wang, X. D. J Appl Polym Sci 2006, 101, 3791.
21. Kirsch, P. Modern Fluoroorganic Chemistry—Synthesis, Reactivity, Applications; Wiley-VCH: New York, 2004.
22. Torres, A. Appl Sur Sci 2007, 254, 1.
23. Bongiovanni, R.; Gianni, A. D.; Priola, A.; Pollicino, A. E. Eur Polym J 2007, 43, 3787.
24. Zhang, Y.; Tan, K. L. Langmuir 2001, 17, 2265.
25. Mcintosh, D.; Valery, N. K.; Barrera, E. Chem Mater 2006, 18, 4561.
26. Toit, F. J. D.; Sanderson, R. D. J Fluorine Chem 1999, 98, 107.
27. Toit, F. J. D.; Sanderson, R. D. J Fluorine Chem 1999, 98, 115.
28. Kingsley, K. C. H.; Graham, B.; George, S.; Natalya, V. P.; Alexander, B. J Fluorine Chem 2007, 128, 1359.
29. Dubois, M.; Guerin, K.; Giirandet, J.; Pilichowsko, J. F.; Thomas, P.; Delbe, K.; Mansot, J. C.; Hamwi, A. Polymer 2005, 46, 6736.

30. Estelrich, A. R.; Ameduri, B.; López-Calahorra, F. Macro Chem Phys 2004, 205, 223.
31. Tressaud, A. J Fluorine Chem 2007, 128, 378.
32. Kharitonov, A. P.; Taege, R.; Ferrier, G.; Teplyakov, V. V.; Syrtsova, D. A.; Koops, G. H. J Fluorine Chem 2005, 126, 251.
33. Peter Hobbs, J.; Philip, B. H.; Michael, R. P. J Fluorine Chem 2000, 104, 87.
34. Huang, H. L.; Yao, Z. H.; Yang, J. H.; Wang, Y.; Shi, D.; Yin, J. H. J Appl Polym Sci 2001, 80, 2538.
35. Yang, J. H.; Yao, Z. H.; Shi, D.; Huang, H. L.; Wang, Y.; Yin, J. H. J Appl Polym Sci 2001, 79, 535.
36. Liu, N. C.; Xie, H. Q.; Baker, W. E. Polymer 1993, 34, 4680.
37. Shi, D.; Yang, J. H.; Yao, Z. H.; Wang, Y.; Huang, H. L.; Wu, J.; Yin, J. H. Polymer 2001, 42, 5549.
38. Yin, J. H.; Zheng, A. N.; Sheng, J. The Reactive Process of Polymers; Science Press: Beijing, 2008.
39. Cartier, H.; Hu, G. H. J Polym Sci Part A: Polym Chem 1998, 36, 1053.
40. Srinivas, S.; Sunggyu, L. J Appl Polym Sci 1998, 70, 1001.
41. Hong, C. K.; Kim, M. J.; Oh, S. H.; Lee, Y. S.; Nah, C. J Ind Eng Chem 2008, 14, 236.
42. Li, Y.; Xie, X. M.; Guo, B. Polymer 2001, 42, 3419.
43. Alexander, L. E. X-ray Diffraction Methods in Polymer Science; Wiley Interscience: New York, 1969; pp 137–145.
44. Owens, D. K.; Wendt, R. C. J Appl Polym Sci 1969, 13, 1741.
45. Peng, S. J.; Zhao, L.; Wu, L. M. Acta Phys Chim Sin 2007, 23, 531.
46. Yang, T. T.; Yao, L.; Peng, H.; Cheng, S. Y.; Park, I. J. J Fluorine Chem 2006, 127, 1105.
47. Kassis, C. M.; Steehler, J. K.; Betts, D. E.; Guan, Z. B.; Romack, T. J.; Desimone, J. M.; Linton, R. W. Macromolecules 1996, 29, 3247.
48. Mo, Z. S.; Zhang, H. F. The Structure of Crystal Polymer and the X-ray Diffraction; Science Publisher: Beijing, 2003; pp 165–170.
49. Yuan, Y. P.; Chen, B.; Zhang, X. Q. Polymer 2007, 48, 5480.
50. Feng, J. C.; Chen, M. C. Polym Int 2003, 52, 42.
51. Zhou, J. J.; Liu, J. G.; Yan, S. K.; Dong, J. Y.; Lin, L.; Chan, C. M.; Schultz, J. M. Polymer 2005, 46, 4077.
52. Lezak, E.; Bartczak, Z.; Galeski, A. Polymer 2006, 47, 8562.
53. Dorina, T. H.; Jozsef, V.; Gottfried, W. E.; Julius Vancso, G. J Polym Sci Part B: Polym Phys 2000, 38, 672.
54. Natu, A. A.; Lofgren, E. A.; Jabarin, S. A. Polym Eng Sci 2005, 45, 400.
55. Yeh, J. T.; Yao, W. H.; Chen, C. C. J Polym Res 2005, 12, 279.
56. Anders, S.; Kenneth, E.; Bengt, S.; Lassas, A. C. J Appl Polym Sci 1996, 59, 1709.
57. Waldman, W. R.; De Paoli, M.-A. Polym Degrad Stab 2008, 93, 272.
58. Pieter, G.; Guido, M.; Giacomo, V. Polym Degrad Stab 1999, 65, 433.
59. Zhu, C.; Guan, W.; Long, H.; Cao, Y.; Liu, X. Plast Rubber Compos 2004, 33, 335.